THE JOURNAL OF PHYSICAL CHEMISTRY B LETTERS

2009, *113,* 8443–8445
Published on Web 06/01/2009

Glassy Dynamics in Nanoconfinement as Revealed by ^{31}P NMR

S. Gradmann, P. Medick, and E. A. Rössler*

Experimentalphysik II, Universität Bayreuth, 95440 Bayreuth, Germany

Received: March 26, 2009; Revised Manuscript Received: May 5, 2009

We investigated the glass former *m*-tricresyl-phosphate confined in different nanoporous silica matrices with defined pore radii from 2−150 nm. While applying different ^{31}P NMR techniques, we were able to detect the extremely stretched correlation functions extending over 7−8 decades in time and reflecting strong dynamic heterogeneities. The experimental results were explained by a topological model for which the broad distribution of correlation times $G(\ln \tau)$ becomes inhomogeneous in space; that is, the "local" dynamics given by a correlation time $\tau(r)$ depend on the distance from the pore center. As $\tau(r)$ changes with temperature, we were able to reintroduce the idea of a dynamic correlation length.

Introduction

Understanding the glass transition is an unsolved problem. Yet, agreement is established that the transition involves cooperative motion which leads to a strong increase of structural relaxation time in the supercooled liquid. Searching for a possible underlying dynamic correlation length, the characteristic molecular slowing-down has been investigated in different types of confining geometries, where the length scale of the confinement may interfere with that of the cooperative motion. Although much information has been compiled, the experimental situation does not allow for a conclusive answer, so far. Approaching the 1−10 nm scale, the dynamics may also show effects from surface interactions, and disentangling both true size and surface effects constitutes a formidable task.[1,2]

Most studies have reported the change of the glass transition temperature T_g or some mean correlation time with the pore size.[2] In addition to a shift in T_g, the distribution of correlation times, $G(\ln \tau)$, is significantly broadened.[3−5] Hence, one wonders if discussing some global or averaged property like T_g or a single correlation time is an appropriate way to describe the change of the dynamics occurring in confinement. Addressing this problem, most detailed information has been gained from molecular dynamics (MD) simulations.[6,7] Here, dynamics can be analyzed spatially resolved, and the correlation times strongly increase when approaching the pore wall. This increase is described by a smooth function of distance, and there is no evidence for some "interfacial phase".[8] Apparently, no size effects are observed; however, the idea of a dynamic correlation length may be reintroduced as the "penetration length" increases while cooling and thus the gradient of correlation times extends more and more into the bulk phase.[7]

This contribution will demonstrate that the scenario presented by MD simulations is compatible with the situation in molecular glass-formers. Exploiting the large time window of ^{31}P NMR and combining results from different NMR techniques,[9,10] we will show that one is able to extract a "distance law" describing the gradient of correlation time in the pores. The approach allows to reproduce the unusually stretched correlation function found for pore radii $R = 2-8$ nm. Moreover, we will estimate the change of the penetration length with temperature and thus providing indeed the possibility to maintain the concept of an increasing dynamic correlation length with decreasing temperature. However, a two-phase model may also work yielding a quite similar spatial extension of the surface effected volume.

Experimental Setup

We investigated the glass former *m*-tricresyl phosphate (m-TCP, cf. Figure 3b) confined in pores with radii reaching from $R = 1.77$ nm up to $R = 150$ nm. Silica matrices with a large aspect ratio of the following types were used as confinement: MCM-41 (Mobil Catalytic Material) and SBA-15 (Santa Barbara) which consist of cylindrical tubes in a hexagonal array, for the pore radii 1.77, 3.61, and 7.25 nm, and CPG (Controlled Porous Glasses, Sigma−Aldrich) with an irregular structure for the larger pores. The MCM and SBA systems were synthesized[1,11] and characterized with well-known methods.[12]

Results

While applying the Hahn echo sequence,[9] we measured ^{31}P NMR spectra. Figure 1 shows on the far left a gradual transition from a solid-state spectrum to a central Lorentzian line within a small temperature interval for the bulk system. In contrast, for the smallest pore radius, we observe the appearance of "two-phase spectra" (far right); they are first recognized for $R = 7.25$ nm. Those two-phase spectra are described by a superposition of a solid-state spectrum $S_{solid}(\omega)$ and a central Lorentzian line $S_{liq}(\omega)$

$$S(\omega, T) = W(T)S_{liq}(\omega) + (1 - W(T))S_{solid}(\omega) \qquad (1)$$

where $W(T)$ designates the weighting factor. Such spectra originate from dynamic heterogeneities which can be described by a broad distribution $G(\ln \tau)$ for which line shape contribution in the intermediate exchange limit ($\tau\delta_{CSA} \cong 1$) can be neglected; here δ_{CSA} denotes the width of the solid-state spectrum. They are characteristic for confined systems[3,5] or binary glass formers.[9] It is important to note that, in the small pores, traces of the

10.1021/jp9027518 CCC: $40.75

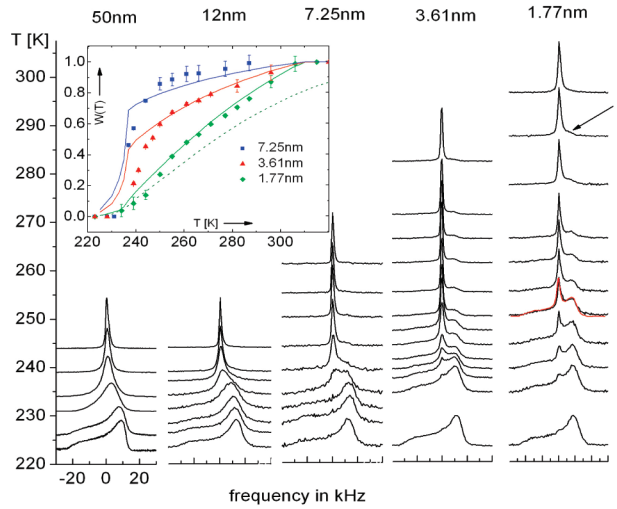

Figure 1. ^{31}P NMR spectra of m-TCP in porous silica with different pore radii; baseline of spectra marks temperature on vertical axis. Insert: weighting factor $W(T)$ (cf. eq 1); dashed line: parameters λ and Δ temperature independent; solid lines: λ temperature dependent (cf. Figure 4).

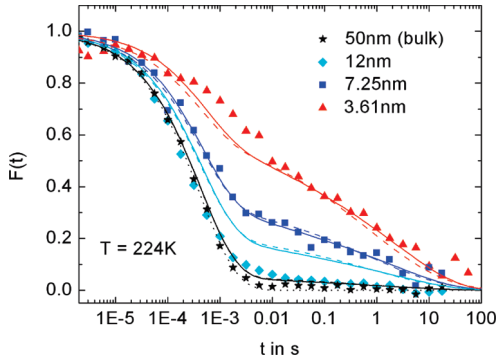

Figure 2. Stimulated echo decays for different pore radii at 224 K. Symbols: experimental data; solid lines: prediction by topological model (cf. eq 2); dashed lines: predictions of two-phase model; dotted line: Kohlrausch fit for bulk TCP.

solid-state spectrum are observed up to high temperatures (cf. arrow in Figure 1) for which in bulk m-TCP only a central line representative of "liquid molecules" is observed. In the pores, in addition to fast reorienting molecules there are molecules which are significantly slowed down. Consequently, $W(T)$ increases more and more slowly for smaller pores as the insert in Figure 1 shows.

As a broad distribution $G(\ln \tau)$ is mapped to a stretched correlation function, we measured the reorientational correlation function directly via the stimulated echo technique.[9] Figure 2 shows a more and more stretched correlation function while going to smaller pore radii at a certain temperature. The bulk data are fitted by a Kohlrausch decay with $\beta = 0.62$ and $\tau_K = 0.42$ ms. By applying ^{31}P NMR, we are able to cover 7−8 decades in time in contrast to other experimental methods, for example, ^{2}H NMR. Obviously, this is necessary to probe the strong dynamic heterogeneities in the confined systems.

To describe quantitatively the correlation functions, we constructed a topological model, which was inspired by simulation work.[6,7] We assumed our porous matrices were composed of cylindrical tubes with a defined radius R. Within these tubes the system can be thought as cut into different shells. Furthermore, we assumed that in each shell the correlation function can be described by a Kohlrausch function with $\beta = 0.62$, as in the bulk, and a mean τ depending on r. The global correlation function $F(t)$ was obtained by a superposition of all single correlation functions, weighted with the corresponding relative volume $v(r)\,dr = 2r/R^2\,dr$

$$F(t) = \int_0^R v(r)\exp\left(-\left[\frac{t}{\tau(r)}\right]^{\beta}\right) dr \qquad (2)$$

$\tau(r)$ denotes the distance law, which introduces a gradient of correlation times to consider surface effects. Molecules next to the wall are slowed down compared to the bulk. As $\tau(r)$ is actually the quantity to be determined, we tried different functions to obtain an optimal interpolation of $F(t)$ for the 7.25 nm sample at 224 K. Finally, eq 3 worked best with $\Delta = 4.85 \times 10^4$ and $\lambda = 0.284$ nm (cf. Figure 2).

$$\tau(r) = \tau_{bulk}\left[1 + (\Delta - 1)\exp\left(-\left[\frac{R - r}{\lambda}\right]^{1.5}\right)\right] \qquad (3)$$

Here, $\tau_{bulk}\Delta$ defines the value of τ at the wall, whereas the penetration length λ determines the range of surface interactions. With these parameters we made predictions for the other pore radii. In Figure 2, one recognizes that the model describes well the change of the correlation function in dependence of R. A better agreement between experiment and model is achieved for smaller pores than for the larger ones. This may be due to the fact that the assumption of cylindrical pores is suitable for the hexagonal geometry of the SBA and MCM samples but not for the irregular structure of the CPG samples. In Figure 3, $\tau(r)$ is plotted (upper red curves). One recognizes a quick rise from τ_{bulk} to a value, which is several magnitudes higher near the wall.

Given the function $\tau(r)$, we are also able to describe the weighting factor $W(T)$ of the spectra (cf. Figure 1). This quantity represents the fraction of molecules which are reorienting fast on the NMR time scale, i.e., $\tau\delta_{CSA} \ll 1$.[13] Thus, $W(T)$ is calculated via integrating the global distribution function $G(\ln \tau)$ up to the limit $\tau_{cut} = 6.6\ \mu s = 1/\delta_{CSA}$. For each shell we assumed a Cole-Davidson distribution $G_{CD}(\ln \tau, \tau_{CD}(r))$ with $\beta_{CD} = 0.51$ and $\tau_{CD} = 1.03$ ms as in the bulk phase that corresponds to a Kohlrausch decay with $\beta_K = 0.62$. All together, this yields

$$W(T) = \int_{-\infty}^{\tau_{cut}} \int_0^R v(r) G_{CD}(\ln \tau, \tau_{CD}(r))\, dr\, d\ln \tau \qquad (4)$$

Furthermore, we had to introduce $\tau(T)$ of the bulk phase. We fit the $\tau(T)$ of bulk m-TCP in a large temperature range (cf. Figure 3b),[10] and included it into our calculation. In fact, the calculated $W(T)$ curve of the 1.77 nm sample (lowest curve) in Figure 1 (inset) shows that we overestimate the confinement effect in our model. Therefore, we introduced a temperature dependence for λ and Δ. By means of analyzing spin−lattice data,[12] we obtained a linear temperature dependence for λ, and while adjusting the so calculated $W(T)$ of the 3.61 nm sample we found $\Delta(T)$. Given this, the interpolation of $W(T)$ for all R is significantly improved (cf. inset Figure 1). As Figure 4 shows, the parameters Δ and λ decrease with increasing temperatures. This is equivalent to an increasing penetration length λ with lowering temperature; the profiles $\tau(r,T)$ are included in Figure 3. At highest temperature the confinement effect essentially disappears whereas close to T_g it is strongest. Following MD simulations,[7] λ may be associated with a dynamic correlation

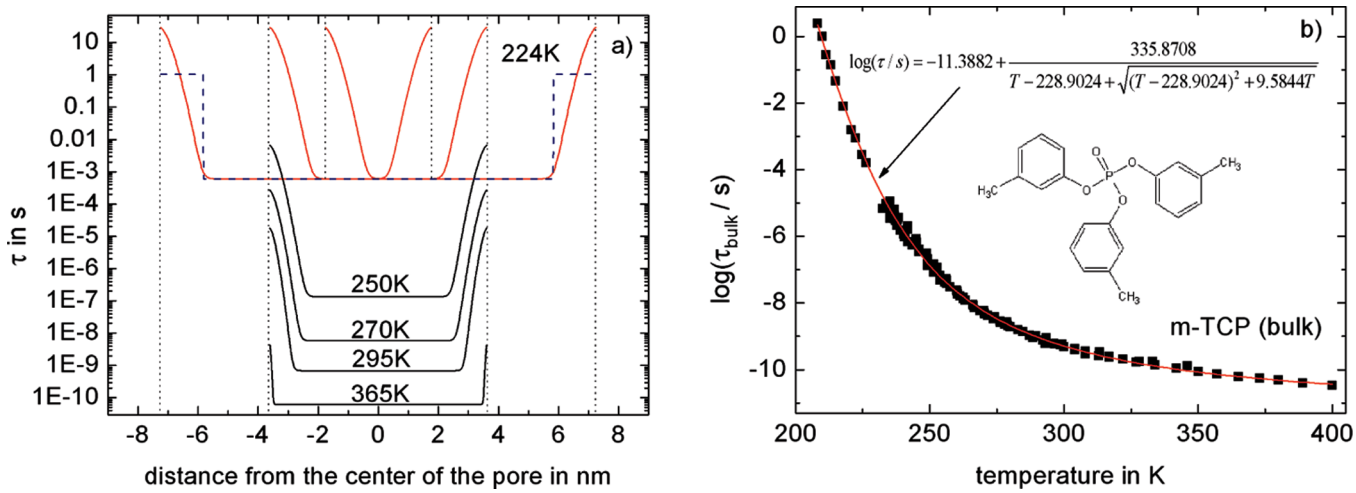

Figure 3. (a) "Distance law" $\tau(r)$ for different pore radii (224 K, red) and temperatures (lower black curves); dashed boxes: two-phase model (7.25 nm, 224 K); (b) $\tau(T)$ dependence of bulk m-TCP together with numerical interpolation.

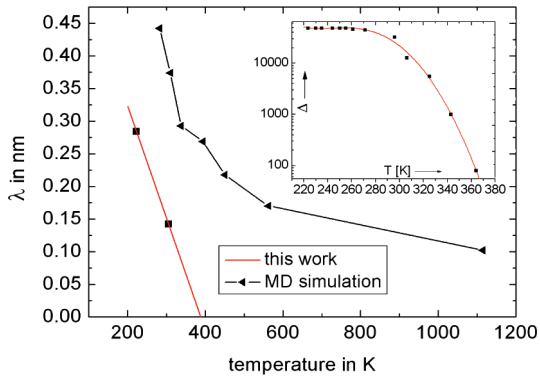

Figure 4. Temperature dependence of the parameters λ ("penetration length") and Δ (inset); λ is compared with a corresponding parameter from MD simulations.[7]

length, and indeed quite similar results are obtained in simulation and the present work (cf. Figure 4). To allow this comparison we used $T_c/T_g = 1.2$ and properties of the simulated LJ liquid ($\sigma_{AA} \triangleq 3.4$ Å for argon, $T_c = 0.435$).[6,14]

Conclusion and Discussion

The good interpolation of our experimental results by the topological model demonstrates that the scenario is compatible with that predicted by MD simulations. A continuous distance law $\tau(r)$ describes well the salient features of the temperature and pore radius dependence of the NMR spectra as well as of the stimulated echo decays. Furthermore, we were able to name the temperature dependence for the parameters λ and Δ. The temperature dependence of the penetration length λ may be associated with a dynamic correlation length that grows with decreasing temperatures in accordance with the MD studies.

In spite of these remarkable results, one can ask if this interpretation is unique. For this reason, we also made a data analysis with a two-phase model. There, we applied a sum of two Kohlrausch functions, one which describes the bulk ($\beta = 0.62$, $\tau_K = 0.42$ ms) and another for the slowed down molecules near the wall ($\beta = 0.30$, $\tau_K = 0.72$s). As Figures 2 and 3a show, we obtained very similar results. Also the thickness of slowed down molecules (about two layers) is essentially the same. Nevertheless, we want to point out, that this approximation only worked with an extremely stretched Kohlrausch function for the molecules near the wall. Therefore, the "wall phase" contains dynamic heterogeneities itself and consequently this scenario comes quite close to our topological model.

Finally, we note that these results became only accessible by applying ^{31}P NMR. Its large time window enabled us to detect characteristic long-time components of the correlation functions in contrast to other experimental methods which could not resolve these features.[15]

Acknowledgment. We thank G. Dosseh and Ch. Alba-Simionesco for the preparation and characterization of the SBA and MCM samples and the DFG Grant RO 907/13-1 for financial support.

References and Notes

(1) Morineau, D.; Xia, Y.; Alba-Simionesco, C. *J. Chem. Phys.* **2002**, *117*, 8966.
(2) *Eur. Phys. J. Special Topics* **2007**, *141*
(3) Lusceac, S. A.; Koplin, C.; Medick, P.; Vogel, M.; Brodie-Linder, N.; LeQuellec, C.; Alba-Simionesco, C.; Rössler, E. A. *J. Phys. Chem. B* **2004**, *108*, 16601.
(4) Arndt, M.; Stannarius, R.; Groothues, H.; Hempel, E.; Kremer, F. *Phys. Rev. Lett.* **1997**, *79*, 2077.
(5) Masierak, W.; Emmler, Th.; Gedat, E.; Schreiber, A.; Findenegg, G. H.; Buntkowsky, G. *J. Phys. Chem. B.* **2004**, *108*, 18890.
(6) Scheidler, P.; Kob, W.; Binder, K. *Europhys. Lett.* **2000**, *52*, 277.
(7) Scheidler, P.; Kob, W.; Binder, K. *Europhys. Lett.* **2002**, *59*, 701.
(8) Gorbatschow, W.; Arndt, M.; Stannarius, R.; Kremer, F. *Europhys. Lett.* **1996**, *35*, 719.
(9) Bingemann, D.; Wirth, N.; Gmeiner, J.; Rössler, E. A. *Macromolecules* **2007**, *40*, 5379.
(10) Rössler, E.; Eiermann, P. *J. Chem. Phys.* **1994**, *100*, 5237.
(11) Brodie-Linder, N.; Dosseh, G.; Alba-Simionesco, C.; Audonnet, F.; Impéror-Clerc, M. *Mater. Chem. Phys.* **2008**, *108*, 73.
(12) Gradmann, S.; Hoff, M.; Medick, P.; Dosseh, G.; Alba-Simionesco, C.; Rössler, E. A. to be published
(13) Rössler, E.; Taupitz, M.; Vieth, H. M. *J. Phys. Chem.* **1990**, *94*, 6879.
(14) Kob, W.; Andersen, H. C. *Phys. Rev. E* **1995**, *51*, 4626.
(15) Streck, C.; Mel'nichenko, Y. B.; Richert, R. *Phys. Rev. B* **1996**, *53*, 5341.

JP9027518